Static properties of an easy-plane ferromagnetic $S=1/2$ chain: Comparison of numerical results and experimental data on $[C_6H_{11}NH_3]CuBr_3$

K. Kopinga
Department of Physics, University of Technology, P.O. Box 513, NL-5600 MB Eindhoven, The Netherlands

T. Delica and H. Leschke
Institut für Theoretische Physik, Universität Erlangen–Nürnberg, D-8520 Erlangen, Federal Republic of Germany

(Received 21 March 1989)

New results of a variant of the numerically exact transfer matrix method have been compared with the experimentally determined static properties of $[C_6H_{11}NH_3]CuBr_3$ (CHAB). Above $T=3.5$ K, the available data on the zero-field heat capacity, the excess heat capacity $\Delta C=C(B)-C(B=0)$ for $B=1$, 2, and 3 T, and the magnetization up to 5 T are described with an accuracy that is comparable to the experimental error. Calculations of the spin-spin correlation functions by this method reveal that the fair description of the experimental correlation length in CHAB by a classical spin model is largely accidental. The zero-field susceptibility deduced from these correlation functions is in satisfactory agreement with the reported data.

I. INTRODUCTION

The static and dynamic properties of one-dimensional (1D) $S=\frac{1}{2}$ systems with a dominant nearest-neighbor interaction have been the subject of a large number of investigations. From a theoretical point of view, these systems are one of the most simple nontrivial many-body systems, displaying a large variety of unexpected features, resulting from the inherent strong fluctuations.[1] Experimentally, several compounds are available that are very good realizations of theoretical model systems. Especially the compound $[C_6H_{11}NH_3]CuBr_3$ (CHAB) has been studied very extensively, since the ferromagnetic intrachain interaction in this system contains about 5% easy-plane anisotropy. In a certain range of temperatures and in-plane magnetic fields, the equation of motion of the spins of this compound can be mapped to a sine-Gordon equation.[2] In this mapping the spins are considered as classical vectors, their motion is confined to the easy (XY) plane and the limit of zero lattice spacing (continuum limit) is taken. The sine-Gordon equation has both linear solutions (magnons) and nonlinear solutions (kink solitons). Despite the fact that the various approximations underlying the mapping to a sine-Gordon model are strictly not valid for CHAB, the behavior of the excess heat capacity $\Delta C=C(B)-C(0)$ of this compound could be fairly well described by this classical model.[3] A more detailed analysis, however, revealed that this largely resulted from an accidental canceling of the quantum effects by the effect of spin-components out of the easy plane.[4] This is one of the observations that triggered more direct calculations of the static and dynamic properties of easy-plane ferromagnetic chain systems based on the original quantum-mechanical spin Hamiltonian.

In this context, various theoretical approaches have been used. First, the thermodynamic properties and the correlation length have been obtained by direct diagonalization of the Hamiltonian matrix for finite systems (typically 11 spins maximum). The properties of the infinite system are evaluated by a suitable extrapolation of the results for these finite chains.[5–7] Alternatively, an appropriate version of the Lie-Trotter product formula[8] is used to rewrite the partition function of the one-dimensional quantum system as a sum over Ising spin variables on a two-dimensional lattice. This sum has been studied for finite lattices using classical Monte Carlo techniques[9,10] or by a numerically exact transfer matrix method.[11] The latter approach, in principle, allows the computation of the properties of chains up to a few hundred spins, thus avoiding the uncertainties introduced by extrapolation of the results for finite chains. On the other hand, results can only be obtained for finite values of the so-called Trotter number m.

The thermodynamic properties of the infinite system obtained from the various approaches have been found to coincide at high temperatures, but at lower T significant differences are found. Recently, a variant of the quantum transfer matrix method has been applied[12,13] in which the internal energy was calculated from the magnetization and all three nearest-neighbor spin-correlation functions in the so-called real-space decomposition. In this way, a better convergence in the Trotter number m has been achieved,[14,15] as was demonstrated by a comparison with exact results. Actually, the internal energy was extrapolated from the results for Trotter numbers $m=7$ and 8 using the $1/m^2$ law.[8,16] In this paper we will compare improved results of this transfer matrix method with experimental data on CHAB, in particular the zero-field heat capacity, the excess heat capacity, the magnetization, and the spin-spin correlations. The numerical procedure itself will be described in detail elsewhere.[17] In Sec. II we will briefly review the crystallographic and magnetic properties of CHAB, giving special attention to the validity of the spin Hamiltonian and the accuracy of

the interaction parameters. In Secs. III–VI we will consider the zero-field heat capacity, the excess heat capacity, the magnetization, and the spin-spin correlations, respectively. The paper will be concluded with a discussion in Sec. VII.

II. $[C_6H_{11}NH_3]CuBr_3$

The crystallographic structure of $[C_6H_{11}NH_3]CuBr_3$ (CHAB) is orthorhombic, space group $P2_12_12_1$.[18] The compound is built up from bibridged linear chains of $CuBr_3^-$ ions running parallel to the c direction. The chains are effectively isolated in the a and b directions by the cyclohexylammonium complexes. From heat-capacity, magnetization,[19] and ferromagnetic resonance[20] experiments, it was deduced that the individual chains in CHAB can be described by the Hamiltonian

$$\mathcal{H}=-2\sum_i (J^{xx}S_i^xS_{i+1}^x+J^{yy}S_i^yS_{i+1}^y+J^{zz}S_i^zS_{i+1}^z)-\mu_B\sum_i \mathbf{S}_i\vec{g}\mathbf{B}\ , \quad (1)$$

with

$$J^{xx}/k_B=55\pm5\ \text{K},\quad (J^{xx}-J^{zz})/k_B=2.75\ \text{K}\ ,$$

and

$$(1-J^{yy}/J^{xx})\simeq 5\times10^{-4}\ .$$

The anisotropy in J/k_B results from the symmetry of the local environment of the Cu^{2+} ions. The y axis coincides with the crystallographic c axis, whereas the x axis lies in the ab plane at an angle φ from the b axis. Two symmetry-related types of chains are present, with $\varphi=-25°$ and $\varphi=25°$, respectively. In this paper we will confine ourselves to measurements collected with the external field $\mathbf{B}\|\mathbf{c}$, which is located in the XY plane for both types of chains. The interchain interactions are smaller than J/k_B by 3 orders of magnitude, and give rise to a three-dimensional long-range ordered state below $T_c=1.50$ K.

The results of measurements of the magnetization and the nuclear spin-lattice relaxation in CHAB could be satisfactorily explained by a model based on the spin Hamiltonian (1) with the set of parameters given previously. In this model the linear excitations were described by standard spin-wave theory, and the nonlinear excitations were associated with sine-Gordon solitons.[21] The small deviations between theory and experimental data were attributed to oversimplifications of the model rather than to uncertainties in the values of the parameters in the spin Hamiltonian. For a meaningful comparison of recent numerical results with experimental data, however, the actual values of the exchange and anisotropy parameters should be established as accurately as possible. This is illustrated by attempts of Wysin and Bishop[11] to improve the agreement between their numerical results and the available data on the excess heat capacity of CHAB by changing the anisotropy parameter $(J^{xx}-J^{zz})/J^{xx}$ from 4% to 10%. Apart from this, the correctness of the spin Hamiltonian (1) has been questioned by Kamieniarz *et al.*[5] because of the lack of agreement between the experimental excess heat capacity and estimates for ΔC based upon the extrapolation of results for finite chains.

With respect to the reported set of parameters of the spin Hamiltonian, we would like to note that the anisotropies $(J^{xx}-J^{yy})/k_B$ and $(J^{xx}-J^{zz})/k_B$ have been determined rather directly by ferromagnetic resonance measurements[20] with an error that most likely does not exceed 0.02 K. Hence the value for the XY anisotropy (2.75 K) may be considered as rather accurate. The small in-plane anisotropy is usually neglected in the calculations. In terms of Zeeman energy, however, this anisotropy corresponds to 0.02 T, which hampers a detailed comparison between theory and experiment at low applied fields. Therefore we have supplemented the reported data on ΔC in the region $B\leq0.65$ T with measurements for $B=1$, 2, and 3 T, at which fields the relative effect of the in-plane anisotropy is expected to be vanishingly small. These new data will be considered in Sec. IV.

The interaction between the chains in CHAB has been estimated from ferromagnetic resonance experiments and the magnetic phase diagram[19,20] as

$$z_FJ_F/k_B=0.08\ \text{K}$$

and

$$z_{AF}J_{AF}/k_B=-0.03\ \text{K}\ .$$

Except very close to T_c and at low values of B, the effect of these interactions is expected to be negligible. The largest uncertainty occurs in the magnitude of the intrachain interaction J/k_B, which has been determined from an analysis of heat-capacity measurements on a polycrystalline sample in the paramagnetic region[19] as

$$J^{xx}/k_B=55\pm5\ \text{K}\ .$$

To check the accuracy of this analysis we have performed additional heat-capacity measurements on a single crystal. The results will be discussed in the next section and compared with an independent estimate of J/k_B from the in-chain magnon dispersion relation.

III. ZERO-FIELD HEAT CAPACITY

Heat-capacity measurements were performed on a single crystal of CHAB with a mass of 527.5 mg for 1.2 K $<T<$ 20.5 K and $B=0$, 1, 2, and 3 T along the crystallographic c axis. The data collected in the presence of a field will be discussed in the next section. The zero-field heat capacity was found to be equal to the data obtained previously on a polycrystalline sample within experimental error (2%), except for the region between 2.5 and 8 K, where the present results are up to 6% lower. This difference may be attributed to impurities present in the polycrystalline material, but may also be caused by the heat of desorption of the ^{3}He exchange gas, used to improve thermal contact within the polycrystalline sample.[19]

The data were analyzed by simultaneous fits of a lattice contribution C_L and a magnetic contribution C_M. For C_L a three-parameter expression appropriate to a chain-

like structure[22] was used. For C_M we used results obtained from a variant of the quantum transfer matrix method[12,13] mentioned in the introduction.

Preliminary fits of C_L+C_M to the data revealed large deviations below $T=6$ K, which were attributed to uncertainties in the theoretical prediction for C_M, since in this temperature region the lattice contribution is relatively small. For this reason, the original numerical method was modified as follows. First, the calculations were also performed for Trotter numbers $m=9$ (and partially $m=10$), and these data were included in the extrapolation. Secondly, the extrapolation in the Trotter number m was improved by taking into account errors in the decomposition of order $1/m^4$. The zero-field heat capacity C_M+C_L obtained in this way, appeared to describe the experimental data down to 3.5 K, with a systematic deviation less than 0.5% for $J^{xx}/k_B=63$ K and an XY anisotropy

$$(J^{xx}-J^{zz})/k_B=2.75 \text{ K} .$$

The results of this fit are plotted in Fig. 1. The squares denote the experimental heat capacity minus the lattice contribution C_L, whereas the solid curve represents the theoretical prediction for C_M. The scatter of the data at higher temperatures results from the fact that in that region $C_L \gg C_M$. Inspection of this figure shows that the systematic deviations between theory and experiment above 3.5 K are smaller than the scatter in the data, demonstrating the excellent quality of the fit. The present value of J^{xx}/k_B agrees completely with the value $J^{xx}/k_B=63\pm3$ K, inferred from fits of the same single-crystal data above $T=7$ K with extrapolated numerical results for finite chains.[7] Since these estimates for J^{xx}/k_B are significantly higher than the value $J^{xx}/k_B=55\pm5$ K obtained from previous measurements on a polycrystalline sample, it is obvious that small errors in the experimental heat capacity may give rise to rather large uncertainties in parameter values obtained from simultaneous fits of C_L and C_M to the data. In our opinion, the present value of J^{xx}/k_B is the most reliable, since it is obtained from fits of accurate theoretical results to single-crystal data down to 3.5 K, where the lattice contribution C_L becomes insignificant. This is corroborated by the fact that this value agrees rather well with the value $J^{xx}/k_B=67\pm2$ K obtained from an analysis of the magnon dispersion relation of deuterated CHAB, measured by inelastic neutron scattering.[23]

Given the nice description of the zero-field heat capacity by the results of the modified quantum transfer matrix method, we have performed similar calculations for the excess heat capacity, the magnetization, and the spin-spin correlations, which will subsequently be discussed in the next sections.

IV. EXCESS HEAT CAPACITY

An analysis of the excess heat capacity $\Delta C=C(B)-C(0)$ has the advantage that experimental errors in the heat capacity of the empty sample holder and the lattice contribution C_L are canceled out. Therefore, it may serve as a rather direct check on the accuracy of theoretical predictions. As already pointed out in Sec. II, the deviations of CHAB from ideal model behavior are expected to be smallest at high fields. For this reason we extended our previous measurements of the heat capacity, which were done at in-plane fields up to 0.65 T and $1.2<T<7$ K, with measurements at $B=1$, 2, and 3 T, and temperatures up to 18 K. The new data on ΔC, obtained by subtracting the experimental zero-field heat capacity from the data collected in the presence of a field, are plotted in Fig. 2. The solid curves reflect the

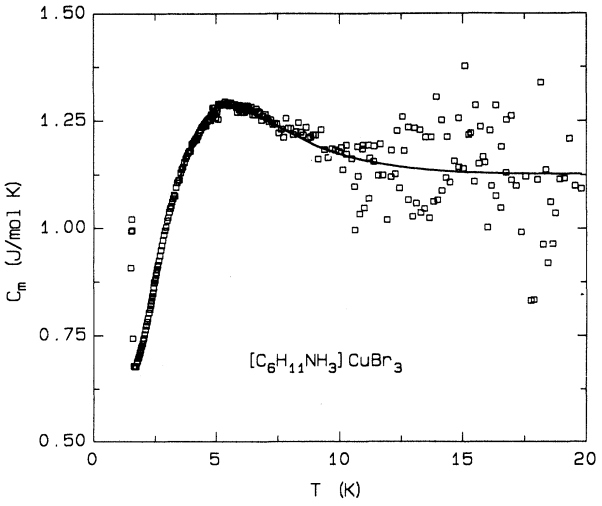

FIG. 1. Temperature dependence of the magnetic heat capacity of CHAB. Squares denote the experimental heat capacity minus the calculated lattice contribution, whereas the solid curve represents the results of the quantum transfer matrix method.

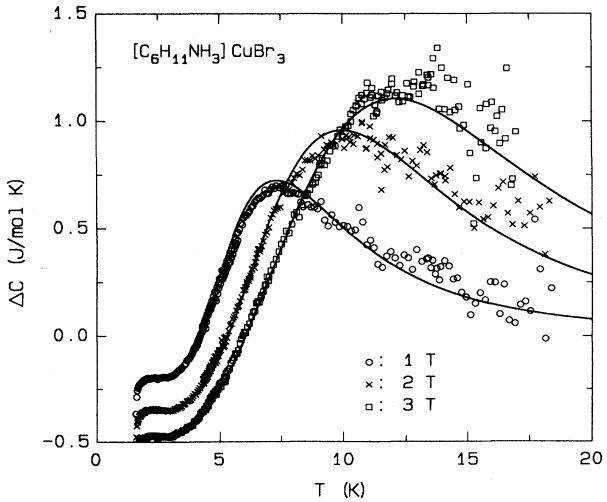

FIG. 2. Excess heat capacity $\Delta C=C(B)-C(B=0)$ of CHAB for $B=1$, 2, and 3 T. The curves denote the corresponding quantum transfer matrix results.

corresponding results of the modified transfer matrix method, discussed in the preceding section. The calculations were performed for the same set of parameters

$$J^{xx}/k_B = 63 \text{ K} ,$$

$$(J^{xx}-J^{zz})/k_B = 2.75 \text{ K}$$

that yielded a good description of the zero-field heat capacity. The g value was taken equal to 2, which is within the range $g_{cc}=2.01\pm0.02$ determined from the saturation magnetization.[21] The curves are drawn in the region where we expect the uncertainty of the extrapolation in the Trotter number m to be smaller than 3%. It is obvious from the figure that not only the heights and positions of the maxima in ΔC are reproduced rather well by the numerical results, but the complete experimental behavior down to 4 K is described correctly. Deviations of up to 5% of ΔC seem to occur at temperatures just below the maximum for $B=1$ and 2 T. If these deviations are actually significant, they most likely result from small inaccuracies of the parameter values in the spin Hamiltonian, since in this region the uncertainty in the numerical extrapolations is much smaller.

It is obvious that our results yield a significant improvement compared with previous calculations of ΔC based on extrapolation of the results for finite chains,[7] especially at temperatures below 10 K. To obtain more information about the applicability of the present theoretical approach, we will discuss in the next section to what extent it describes the experimentally observed magnetization.

V. MAGNETIZATION

The magnetization of CHAB in external fields up to 5 T along the crystallographic c axis, which is located in the easy XY plane, has been determined previously for 1.4 K $\leq T \leq$ 10 K.[21] In this section we will subsequently focus our attention to the low- and high-field region.

The magnetization measured in fields up to $B=2$ T is plotted in Fig. 3 as M/M_S against B, where M_S denotes the saturation magnetization. The different symbols reflect sets of measurements performed at different temperatures. The solid curves reflect the corresponding behavior calculated from the modified quantum transfer matrix method for $T \geq 3$ K, where we estimate the accuracy of the numerical extrapolations to be better than a few percent. In these calculations we used the same set of parameters as in the preceding sections, i.e.,

$$J^{xx}/k_B = 63 \text{ K} ,$$

$$(J^{xx}-J^{zz})/k_B = 2.75 \text{ K} ,$$

$$g_{cc} = 2 .$$

Inspection of this figure shows an almost perfect agreement between the experimental data and the numerical results; for most temperatures, the deviations do not exceed the experimental error in the determination of M ($\sim$2%). Around 1 T, the data for 4.2, 5, and 6 K seem to be slightly lower than the correspondent theoretical predictions. Since in this region $\partial M/\partial T$ is rather large, these systematic deviations should most likely be attributed to errors in the temperature measurement, because in our magnetometer the sample temperature may incidentally be 50–100 mK higher than that of the reference thermometer.

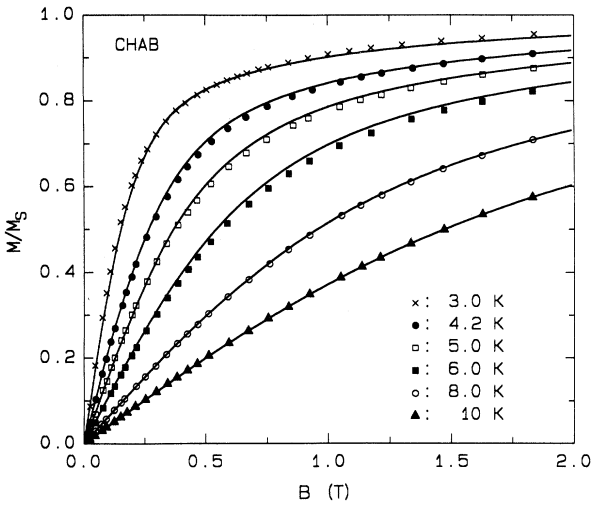

FIG. 3. Reduced magnetization of CHAB for B||c at various temperatures. The curves denote the corresponding quantum transfer matrix results.

In order to investigate the behavior at high fields in more detail, we plotted M/M_S against $1/\sqrt{B}$ in Fig. 4. The more usual reduced form, i.e., M/M_S against $T/\sqrt{B}$, was not chosen, since in that case the majority of the data would collapse on one single curve,[21] which would hamper a detailed comparison between theory and the data. Figure 4 corresponds to the field region be-

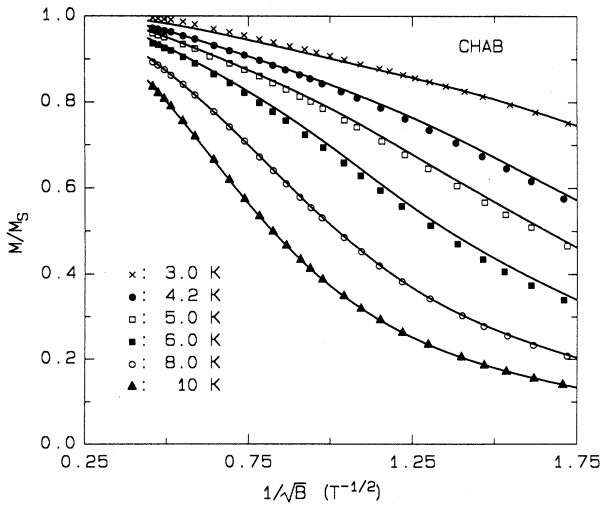

FIG. 4. High-field part of the magnetization of CHAB for B||c plotted as M/M_S against $1/\sqrt{B}$ at various temperatures. The curves denote the corresponding transfer matrix results.

tween 0.4 and 5 T. It is obvious that also in this region an almost perfect agreement between the available data and the transfer matrix results occurs. A fair overall description of the magnetization of CHAB has also been obtained from quantum Monte Carlo calculations and extrapolated results for finite chains.[10] Especially at low fields and temperatures, however, the latter results significantly deviate from the experimental data.

VI. SPIN-SPIN CORRELATIONS

The in-chain spin-spin correlation length in deuterated CHAB has been measured with quasielastic neutron scattering.[24] In the paramagnetic region, the correlations within the individual (decoupled) chains give rise to diffuse planes within reciprocal space perpendicular to the chain direction. The width of these planes is roughly proportional to the inverse correlation length κ.[25] In general, κ is deduced from the measurements by fitting the intensity observed in scans perpendicular to such a plane with a Lorentzian

$$I(q)=\frac{A\kappa}{q^2+\kappa^2} . \tag{2}$$

In this equation q denotes the component of the scattering vector perpendicular to the plane, and A is a proportionality factor. In most cases a constant background intensity is included in the fit.

Formally, Eq. (2) is only valid if q is small compared to the width of the Brillouin zone along the chain direction and if the spin-spin correlations decay exponentially with distance. Since in the limit of large distance the latter condition usually holds, κ is often deduced from the two-spin correlation function $\rho_n^\alpha=\langle S_i^\alpha S_{i+n}^\alpha\rangle$, $\alpha=x,y,z$, using the relation

$$\kappa_\alpha=\lim_{n\to\infty}\left(\ln|\rho_n^\alpha/\rho_{n+1}^\alpha|\right) . \tag{3}$$

This approach has the drawback that it is not very suitable for procedures based on direct diagonalization of the Hamiltonian for finite chains, given the limited maximum number of spins ($N=11,12$). Apart from this, the small magnitude of ρ_n^α for large n may introduce numerical complications. These can be avoided by using a more general definition of the inverse correlation length in zero field given by[26]

$$(\kappa_\alpha)^2=2\lim_{N\to\infty}\left[\sum_{n=-N}^{N}\langle S_0^\alpha S_n^\alpha\rangle\left[\sum_{n=-N}^{N}n^2\langle S_0^\alpha S_n^\alpha\rangle\right]^{-1}\right] . \tag{4}$$

The differences between the values of κ obtained from Eq. (3) or Eq. (4), respectively, are negligible at low temperatures. The latter equation has been used in previous transfer matrix calculations on classical spin chains.[27] For CHAB, such calculations yielded a fair description of the experimental data,[24] provided that the classical spin length $\tilde{S}$ was chosen equal to S instead of $\sqrt{S(S+1)}$. It is obvious that Eq. (4) can also be used to deduce estimates for κ from numerical computations of ρ_n^α for quantum systems with finite N.

Recently, the temperature dependence of κ_x for CHAB has been calculated from finite chain extrapolations and by quantum Monte Carlo techniques.[10] Although both the uncertainty in the experimentally deduced correlation length and the computed values of κ_x is rather large, the theoretical predictions for $T>4$ K are systematically lower than the data by a factor of 2. In order to get more information about the origin of this discrepancy, we have calculated the temperature dependence of κ_x using our modified quantum transfer matrix method, which we expect to be rather accurate, in view of the results presented in the preceding sections.

First, $\langle S_0^x S_n^x\rangle$ was calculated for $1\le n\le 50$ and a chain of 150 spins, where $\mathbf{S}_0$ was located near the center of the chain. The dependence of $\langle S_0^x S_n^x\rangle$ on n is plotted in Fig. 5 for $n\ge 1$ and several temperatures in the range 2.5 K $\le T\le 10$ K. Since the spin quantum number $S=\frac{1}{2}$, the autocorrelation functions $\langle(S_n^\alpha)^2\rangle$ are exactly equal to $\frac{1}{4}$ for $\alpha=x,y,z$, all n, and all temperatures. The obvious discontinuity of $\langle S_0^x S_n^x\rangle$ for $n=0$ at finite temperatures should be attributed to the quantum nature of the present system, since it is not present in the results for chains of classical spins.[27] Inspection of Fig. 5 shows also that, especially for $n\le 10$ and low T, significant deviations from exponential behavior occur, and hence the use of long chains in the calculations of κ seems essential.

Next, κ_x was calculated from the two-spin correlation functions using the relation $\langle S_0^x S_n^x\rangle=\langle S_0^x S_{-n}^x\rangle$ and Eq. (4). The correlation functions for $n>50$ were estimated by extrapolation of $\langle S_0^x S_n^x\rangle$, assuming exponential behavior at large n. The inclusion of these extrapolated data in Eq. (4) resulted in a decrease of the calculated value of κ_x of $\sim 10\%$ at $T=2.5$ K, whereas at 7 K this decrease was less than 1%. Between 4 and 12 K, the correlation length

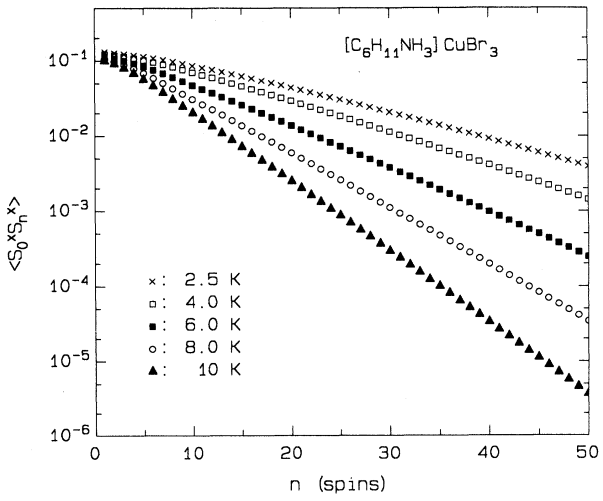

FIG. 5. The correlation functions $\langle S_0^x S_n^x\rangle$ for the easy-plane spin components in CHAB calculated by the quantum transfer matrix method for various temperatures. The autocorrelation function $\langle S_0^x S_0^x\rangle$, which is not included in the figure, is equal to $\frac{1}{4}$ for all temperatures.

obtained in this way agrees with the reported results[10] within the quoted errors of about 15%. If the latter results are corrected for the fact that in the corresponding calculations a value of $J^{xx}/k_B = 55$ K has been used instead of the present value $J^{xx}/k_B = 63$ K, they predict a more or less constant value of κ/T equal to 0.023 ± 0.004, in rather good agreement with the present calculations. This strongly suggests that the origin of the discrepancy between theory and experiment must be sought in the interpretation of the experimental data. In this respect we like to recall that in the instrumental configuration used for the quasielastic neutron scattering experiments both the in-plane and out-of-plane spin components were measured simultaneously. In view of the results of a classical spin model, it was assumed that at $T > 8$ K the correlations of the in-plane (x) and out-of-plane (z) spin-components were equal. Since, on the other hand, below $T = 3$ K the contribution of the out-of-plane spin components near $q = 0$ was negligible, the experimental intensity profile was fitted with a single Lorentzian.

To check the validity of this approach, we have calculated the temperature dependence of both κ_x and κ_z in the region 2.5 K $\leq T \leq 50$ K. The results are plotted as κ/T against T in Fig. 6, together with the reported experimental data[24] and the predictions from a classical spin model with $\tilde{S} = \frac{1}{2}$, calculated for the same set of exchange and anisotropy parameters. The quantum transfer matrix results presented in this figure indicate that the "crossover" from isotropic (Heisenberg) behavior at high T to anisotropic (XY-like) behavior at low T occurs at much higher temperatures than suggested by the classical spin model, which complicates the interpretation of the neutron scattering data. Therefore we have chosen a more

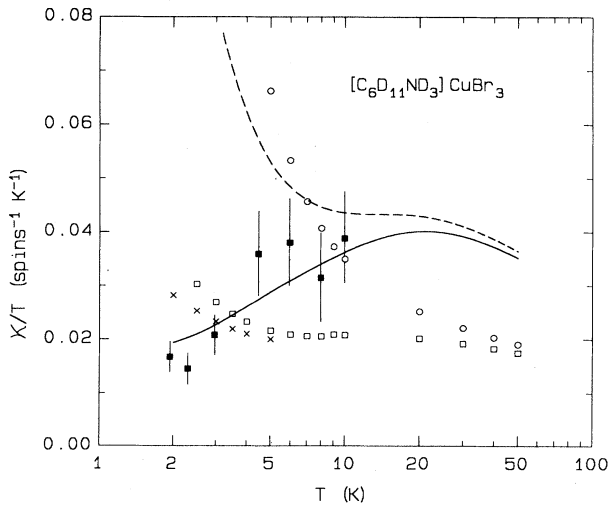

FIG. 6. Inverse correlation length in CHAB plotted as κ/T against T. Solid squares represent the reported neutron scattering results Ref. 24. The solid and dashed curves represent the classical spin predictions for the in-plane and out-of-plane spin components, respectively. The quantum transfer matrix results for the in-plane and out-of-plane spin components are denoted by open squares and circles, respectively. The crosses reflect the effect of a small in-plane anisotropy.

direct comparison of the results of our numerical computations with the experimental data by directly calculating an intensity distribution $\mathcal{S}^{\alpha}(q)$, $\alpha = x,y,z$, in analogy to[26]:

$$\mathcal{S}^{\alpha}(q) = \sum_{n=-N}^{N} e^{-iqn} \langle S_0^{\alpha} S_n^{\alpha} \rangle \ . \tag{5}$$

The calculated intensities for the easy (x), intermediate (y), and hard (z) spin components were added together with weight factors corresponding to the experimental conditions,[24] i.e., 0.28, 1.0, and 0.72, respectively. This combination appeared to describe the experimentally observed scattering profile with an error sum comparable to that of the single Lorentzian used in the original interpretation. Unfortunately, the large statistical uncertainties of the data did not allow more pertinent conclusions.

Next, we will return to the region below $T = 4$ K. In contrast to the experimental data, presented in Fig. 6, the calculated values of κ_x/T increase at lower temperatures. Although the same tendency has been observed in recent quantum Monte Carlo simulations,[10] it cannot *a priori* be excluded that this is an artifact of the present numerical approach. In this respect we like to note that the accuracy of the calculated correlation functions $\langle S_0^{\alpha} S_n^{\alpha} \rangle$ decreases at larger n, since in that region the error in the extrapolation in the Trotter number m increases. Especially at low temperatures, where the long-range correlations are important, this may have a significant effect on the calculated value of κ. On the other hand, the more rapid decrease of the experimental inverse correlation length may also be caused by the small anisotropy within the XY plane. In our quantum transfer matrix calculations up till now this anisotropy (~ 0.02 K) has been neglected, although the results of a classical spin model[24] suggest that it may become important in this temperature region. To investigate this point, we calculated the temperature dependence of κ_x including an in-plane anisotropy of 0.02 K, i.e.,

$$J^{xx}/k_B = 63.02 \text{ K} \ ,$$

$$J^{yy}/k_B = 63.0 \text{ K} \ ,$$

and

$$J^{zz}/k_B = 60.25 \text{ K} \ .$$

The resulting values for κ_x/T are also plotted in Fig. 6. It is obvious from this figure that the inclusion of even such a small amount of anisotropy induces a substantial decrease of κ_x below $T = 5$ K. We did not try to increase the in-plane anisotropy such that our numerical results yielded a more precise description of the data at low temperatures. As already mentioned, the absolute accuracy of the numerical results rapidly decreases as T goes to zero, whereas, on the other hand, a substantial part of this anisotropy is of dipolar origin and hence cannot properly be accounted for by the spin Hamiltonian (1).

VII. DISCUSSION

The comparison of the experimental data on the thermodynamic properties of CHAB with the results of the

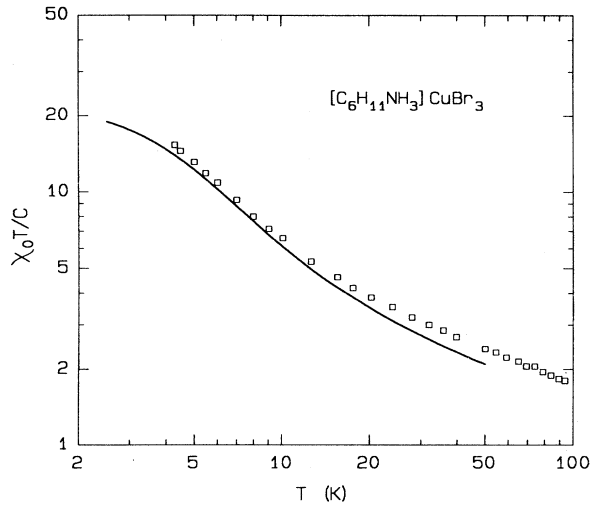

FIG. 7. Temperature dependence of the zero-field susceptibility of CHAB. Squares denote experimental data taken from Ref. 28, whereas the solid curve reflects the quantum transfer matrix result.

modified quantum transfer matrix method, presented in Sec. III, IV, and V, reveals an almost perfect agreement for temperatures down to 3 K. The minor deviations that are observed incidentally can largely be explained by experimental errors or small uncertainties in the precise value of the parameters in the spin Hamiltonian.

With respect to the correlation length, the available experimental data do not allow a meaningful test of the accuracy of the corresponding numerical results, as was outlined in the preceding section. Nevertheless, our numerical results for the correlation functions allow a direct computation of the quasielastic neutron scattering intensities. Moreover, the results for $\langle S_0^\alpha S_n^\alpha \rangle$ can be used for a direct calculation of the magnetic susceptibility per spin, which can be expressed as

$$\chi_0^{\alpha\alpha} = \lim_{N\to\infty} \frac{g^2\mu_B^2}{k_B T} \sum_{n=-N}^{N} \langle S_0^\alpha S_n^\alpha \rangle \ . \tag{6}$$

The resulting prediction can be compared rather directly with the experimentally determined zero-field susceptibility of CHAB.[28] We will confine ourselves to the reported data for the susceptibility along the c axis, which corresponds to the y axis in the spin Hamiltonian (1). In Ref. 28 the susceptibility is given as $\chi_0 T/C$ against T, where C denotes the Curie constant,

$$C = Ng^2\mu_B^2 S(S+1)/3k \ .$$

In the analysis a value $g_{cc}=2.23$ was used. We have reproduced these data between 4 and 100 K in Fig. 7, after rescaling in such a way that $g_{cc}=2.01$, in accordance with the magnetization measurements[21] quoted in Sec. V. The solid curve represents the corresponding theoretical prediction, calculated from Eq. (6), using the same set of exchange and anisotropy parameters as in the preceding sections. The small in-plane anisotropy is neglected, since it has almost no effect in the present temperature region. Inspection of the figure shows that the overall behavior of the data is described rather well by the numerical results. In the temperature region up to $\sim$20 K, the theoretical prediction is systematically lower than the data by a constant factor of about 6%. As already mentioned in the preceding section, the accuracy of the extrapolation in the Trotter number m rapidly increases at higher T. Therefore we believe that this constant deviation should be attributed to the small uncertainty in the g value, which enters quadratically in χ, or to a systematic error in the experimental determination of the susceptibility. At higher temperatures, the deviations between theory and experiment increase, which can be explained by the effect of temperature-independent paramagnetism, for which the reported experimental data have not been corrected.[28]

Concluding we would like to remark that in most calculations an increase of the chain length from $N=150$ to 300 was found to have only minor effects,[13] even at $T=3$ K, corresponding to a reduced temperature

$$kT/2JS(S+1)=0.02 \ .$$

Our analysis of the zero-field heat capacity indicated that extension of the calculations to lower temperatures would probably require an increase of the chain length N, but, more definitely, an increase of the maximum Trotter number m. In this respect we note that calculations of $\langle S_0^x S_n^x \rangle$ for a chain of 500 spins and $T=3$ K yielded results that are, up to $n=50$, equal to those of similar calculations for $N=150$. This demonstrates again that the numerical results presented in this paper are hardly affected by the finite length of the chain.

ACKNOWLEDGMENTS

This work was supported in part by the Deutsche Forschungsgemeinschaft. Part of the research was carried out at the Center of Simulational Physics at the University of Georgia, whereas the final computations were performed at the Cyber 205 of the HFK Karlsruhe. We would like to thank W. J. M. de Jonge for stimulating discussions and G. C. de Vries and J. Emmen for their help in the analysis of the experimental data.

[1]See, for instance, G. Müller, Z. Phys. B **68**, 149 (1987), and references therein.

[2]H. J. Mikeska, J. Phys. C **11**, L29 (1978); **13**, 2913 (1980); E. Magyari and H. Thomas, *ibid.* **15**, L333 (1982).

[3]K. Kopinga, A. M. C. Tinus, and W. J. M. de Jonge, Phys. Rev. B **29**, 2868 (1984).

[4]A. M. C. Tinus, W. J. M. de Jonge, and K. Kopinga, Phys. Rev. B **32**, 3154 (1985).

[5]G. Kamieniarz and C. VanderZande, Phys. Rev. B **35**, 3341 (1987).

[6]G. Kamieniarz, Solid State Commun. **66**, 229 (1988).
[7]K. Kopinga, J. Emmen, G. C. deVries, L. F. Lemmens, and G. Kamieniarz, J. Phys. (Paris) Colloq. **50**, Suppl. 12, C8-1451 (1989).
[8]M. Suzuki, Prog. Theor. Phys. **56**, 1454 (1976).
[9]I. Satija, G. Wysin, and A. R. Bishop, Phys. Rev. B **31**, 3205 (1985).
[10]G. Kamieniarz, F. Mallezie, and R. DeKeyser, Phys. Rev. B **38**, 6941 (1988).
[11]G. M. Wysin and A. R. Bishop, Phys. Rev. B **34**, 3377 (1986).
[12]T. Delica, Phys. Rev. B **37**, 9879 (1988).
[13]T. Delica, R. W. Gerling, and H. Leschke, J. Phys. (Paris) Colloq. **50**, Suppl. 12, C8-1585 (1989).
[14]H. Betsuyaku, Phys. Rev. Lett. **53**, 629 (1984); Prog. Theor. Phys. **73**, 319 (1985).
[15]H. de Raedt, A. Lagendijk, and J. Fivez, Z. Phys. B **46**, 261 (1982).
[16]R. M. Fye, Phys. Rev. B **33**, 6271 (1986); R. M. Fye and R. T. Scalettar, *ibid.* **36**, 3833 (1987).
[17]T. Delica and H. Leschke (unpublished).
[18]G. C. de Vries, R. B. Helmholdt, E. Frikkee, K. Kopinga, W. J. M. de Jonge, and E. F. Godefroi, J. Phys. Chem. Solids. **48**, 803 (1987).
[19]K. Kopinga, A. M. C. Tinus, and W. J. M. de Jonge, Phys. Rev. B **25**, 4685 (1982).
[20]A. C. Phaff, C. H. W. Swüste, W. J. M. de Jonge, R. Hoogerbeets, and A. J. van Duyneveldt, J. Phys. C **17**, 2583 (1984).
[21]K. Kopinga, A. M. C. Tinus, W. J. M. de Jonge, and G. C. de Vries, Phys. Rev. B **36**, 5398 (1987).
[22]K. Kopinga, P. van der Leeden, and W. J. M. de Jonge, Phys. Rev. B **14**, 1519 (1976).
[23]G. C. de Vries, E. Frikkee, K. Kakurai, M. Steiner, B. Dorner, K. Kopinga, and W. J. M. de Jonge, Physica B **156&157**, 266 (1989).
[24]K. Kopinga, W. J. M. de Jonge, M. Steiner, G. C. de Vries, and E. Frikkee, Phys. Rev. B **34**, 4826 (1986).
[25]M. Steiner, J. Villain, and G. C. Windsor, Adv. Phys. **25**, 87 (1976).
[26]J. M. Loveluck, S. W. Lovesey, and S. Aubry, J. Phys. C **8**, 3841 (1975).
[27]F. Boersma, K. Kopinga, and W. J. M. de Jonge, Phys. Rev. B **23**, 186 (1981).
[28]R. Hoogerbeets, E. H. Abu Bakr, and A. J. van Duyneveldt, Physica B **128**, 161 (1985).